

TOGAC17_MSD_R_StabilityFBandFFApproach.docx

This report discusses the replication of the control systems from the work of Aydin et al. (2020) from the paper Towards Collaborative Drilling with a Cobot Using Admittance Controller and Stienen et al. (2018) Admittance control for physical human–robot interaction. It shows the control designs along with their transfer functions. After reviewing the design of the research controllers, our feedback and feedforward and feedforward linearization controllers are analyzed similarly (although the feedforward controller will not be implemented in our system).

Stability maps for the feedback controller and feedforward controller were derived and are shown here.

Contents

1. Previous Literature Controller Designs	2
Closed Loop Transfer Functions and Control Systems: From “Towards Collaborative Drilling with a Cobot Using Admittance Controller”	2
Closed Loop Transfer Functions and Control Systems: From “Admittance control for physical human–robot interaction”	3
2. Controller designs for our controllers	4
Feedback Control System for Velocity Control of Basic Mass Spring Damper:	4
Feedback with Feedforward for Velocity Control of Basic Mass Spring Damper:.....	5
3. Open Loop Transfer Functions:	6
4. Stability identification Methods:.....	7
5. Mass Spring Damper Systems:	7
6. Key Terms/Abbreviations:	11
7. Normalized Stability analysis of Plant dynamics with an applied admittance controller and impedance bounds.....	11
8. Normalized Stability Results: Feedback	12
9. Normalized Stability Results: Feedback with Feedforward and Linearization	14

1. Previous Literature Controller Designs

Closed Loop Transfer Functions and Control Systems: From “Towards Collaborative Drilling with a Cobot Using Admittance Controller”

Aydin et al (2020)

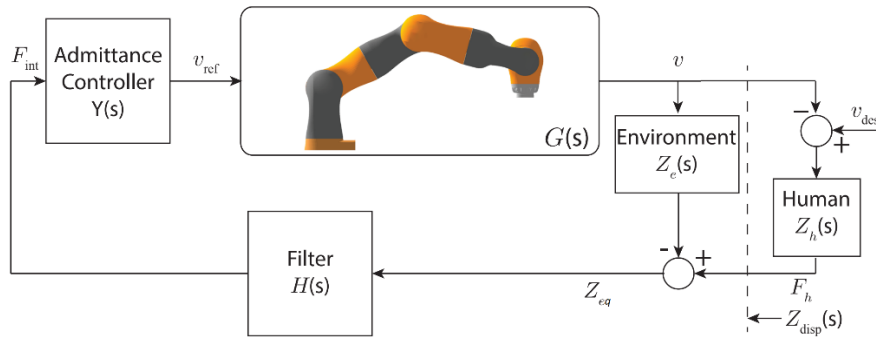


Figure 1 Basic Admittance Control System for Cobot [1]

Resultant Transfer Function:

$$T1(s) = \frac{V(s)}{F_{ref}(s)} = \frac{G(s)Y(s)}{1+G(s)Y(s)H(s)Z_{eq}(s)} \quad Eq 1$$

Closed Loop Transfer Functions and Control Systems: From “Admittance control for physical human–robot interaction”

Stienen et al (2020)

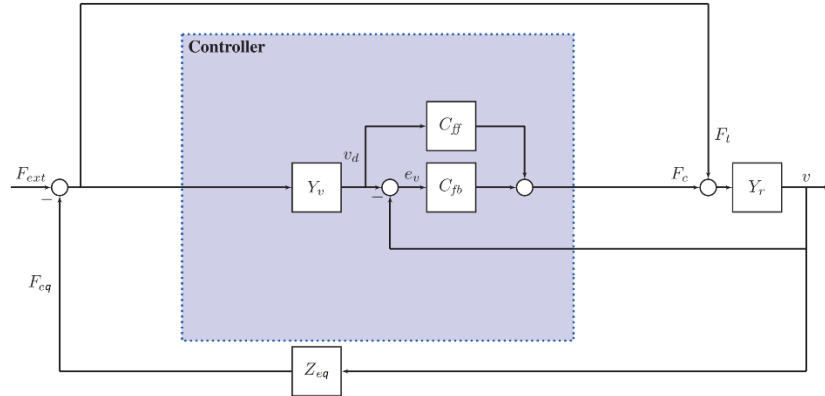


Figure 2 Basic Admittance Control System for Feedforward and Plant Linearization [2]

Resultant Transfer Function:

$$T2(s) = \frac{V(s)}{F_{ext}(s)} = \frac{Yr(s)(C_{fb}(s)Yv(s)+C_{ff}(s)Yv(s)+1)}{Yr(s)(Zeq(s)+C_{fb}(s)(Yv(s)Zeq(s)+1)+C_{ff}(s)Yv(s)Zeq(s))+1} \quad Eq 2$$

2. Controller designs for our controllers

Feedback Control System for Velocity Control of Basic Mass Spring Damper:

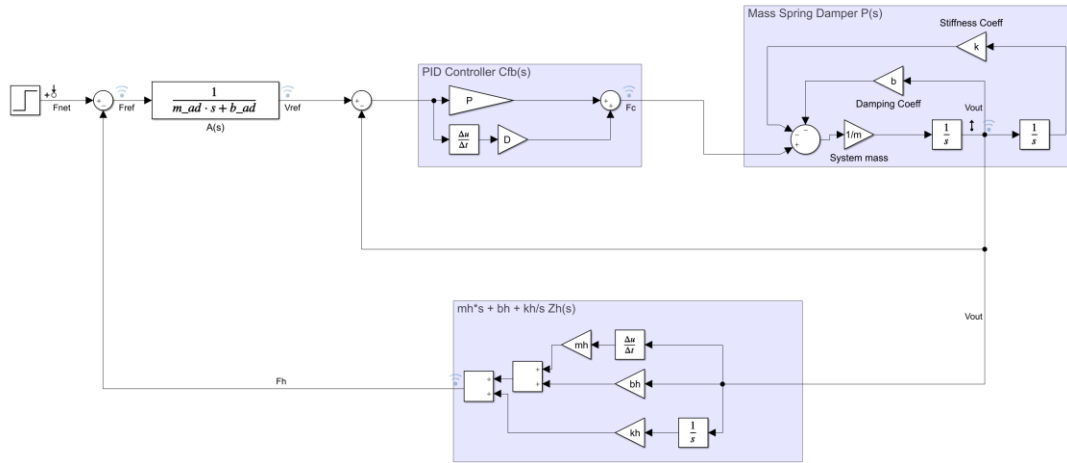


Figure 3 Admittance Control System for Feedback Controller

Resultant Transfer Function:

$$T3(s) = \frac{V(s)}{F_{net}(s)} = \frac{A(s)C_{fb}(s)P(s)}{1 + C_{fb}(s)P(s)(A(s)Z_{eq}(s) + 1)} \quad Eq 3$$

Feedback with Feedforward for Velocity Control of Basic Mass Spring Damper:

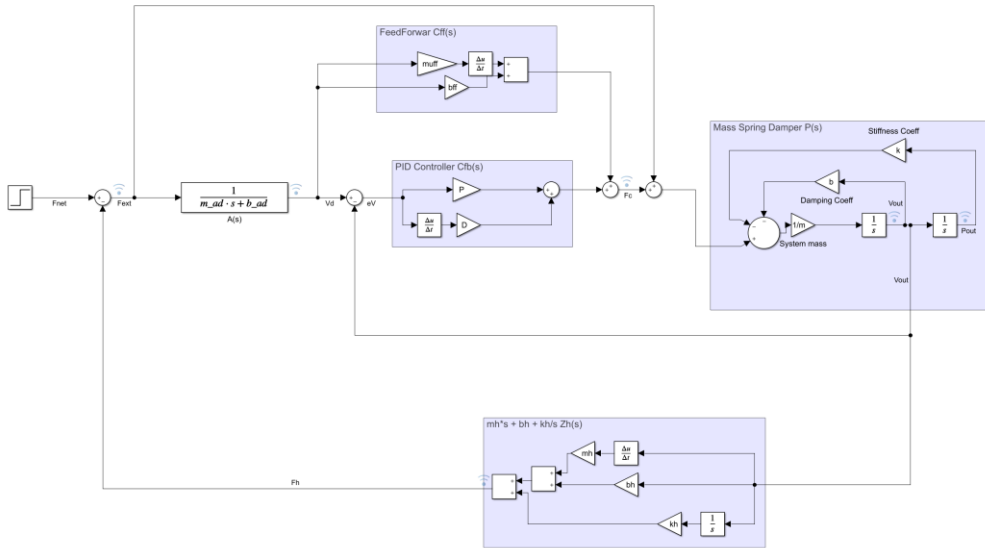


Figure 4 Admittance Control System for a Feedback Controller with Feedforward and Plant Linearization

Resultant Transfer Function:

$$T4(s) = \frac{V(s)}{F_{net}(s)} = \frac{P(s)(A(s)C_{fb}(s) + A(s)C_{ff}(s) + 1)}{P(s)(Zeq(s) + C_{fb}(s)(A(s)Zeq(s) + 1) + A(s)C_{ff}(s)Zeq(s)) + 1} \quad Eq 4$$

Notation Unified For Transfer Functions:

The above transfer functions for all the controllers use different notation to represent the same parameters. Here the equations 1 through 4 are unified with the same notation for simplification.

$$T1(s) = \frac{V(s)}{F_{net}(s)} = \frac{GA}{1 + GAHZeq}$$

$$T2(s) = \frac{V(s)}{F_{net}(s)} = \frac{P(AC_{fb} + AC_{ff} + 1)}{P(Zeq + C_{fb}(AZeq + 1) + C_{ff}AZeq) + 1}$$

$$T3(s) = \frac{V(s)}{F_{net}(s)} = \frac{AC_{fb}P}{1 + C_{fb}P(AZeq + 1)}$$

$$T4(s) = \frac{V(s)}{F_{net}(s)} = \frac{P(AC_{fb} + AC_{ff} + 1)}{P(Zeq + C_{fb}(AZeq + 1) + AC_{ff}Zeq) + 1}$$

3. Open Loop Transfer Functions:

The open loop transfer functions were also isolated from our controller design. Open Loop Transfer functions for the Controller in figure 3 (fb) and the controller in figure 4 (ff) for mass spring damper systems.

$$T5(s) = \frac{F_{eq}(s)}{F_{net}(s)} = \frac{AC_{fb}PZeq}{PC_{fb}+1} \quad Eq 5$$

$$T6(s) = \frac{F_{eq}(s)}{F_{net}(s)} = \frac{(A(C_{fb}+C_{ff})+1)PZeq}{PC_{fb}+1} \quad Eq 6$$

4. Stability identification Methods:

The stability of the above transfer functions was tested by using the following methods from the previous literature. Different admittance mass and damping values were applied iteratively to map out what values of m_{ad} and b_{ad} were able to keep the system stable.

Aydin et al. : Closed Loop Poles of T(s) with root locus

Stienen et al. : Open Loop Phase of $\frac{F_{eq}}{F_{net}} = Y_a Z_{eq}$

See the papers for a more detailed explanation of the stability methodology

The method from Stienen et al. was applied to the Controller in figure 3 (fb) and the controller in figure 4 (ff) for mass spring damper systems in the analysis shown below here.

5. Mass Spring Damper Systems:

System properties used to build the plants and controllers for the Mass Spring Damper system used in the stability analysis.

$m = 10$; %kg System mass for MSD Ps

$b = 5$; %Ns/m System damping for MSD Ps

$k = 1$; %N/m System stiffness for MSD Ps

$P = 900$; %Ns/m Proportional gain for controller Cs

$D = 10$; % Derivative gain for controller Cs

Several different conditions of a mass spring damper were applied for completeness. Given that a mass spring damper is a simple second order system, the different cases for mass spring and damping values will give us a general idea of the expected response. We produced 6 different systems labeled in the figures(5 and 6) below in which we would select the mass spring damper that most closely resembles the performance we would want out of the real robot.

See `plant_dynamics_select.m` for more information. Each system contained the following parameters.

%System 1 Under Damped

m = 10;
b = 5;
k = 1;

%System 2 Critically Damped

m = 10;
b = 2*0.3162*m;
k = 1;

%System 3 Undamped

m = 10;
b = 0;
k = 1;

%System 4 Over Damped

m = 10;
b = 10;
k = 1;

%System 5 No Stiffness Critically Damped

m = 10;
b = 2*0.3162*m;
k = 0;

%System 6 No Stiffness or Damping mass system (double integrator)

m = 10;
b = 0;
k = 0;

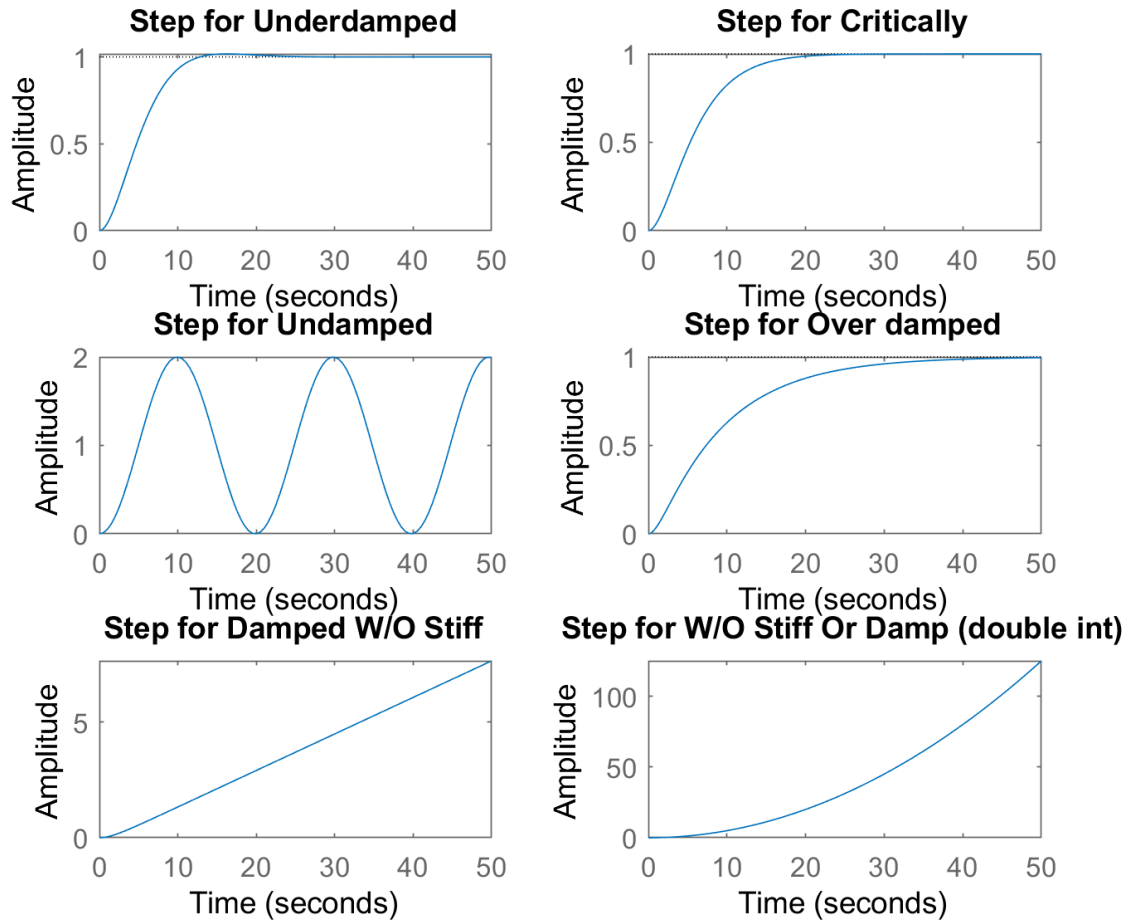


Figure 5 Position input response of a mass spring damper

The position response for a mass spring damper can be seen above for different cases of m , b and k for the mass spring damper system.

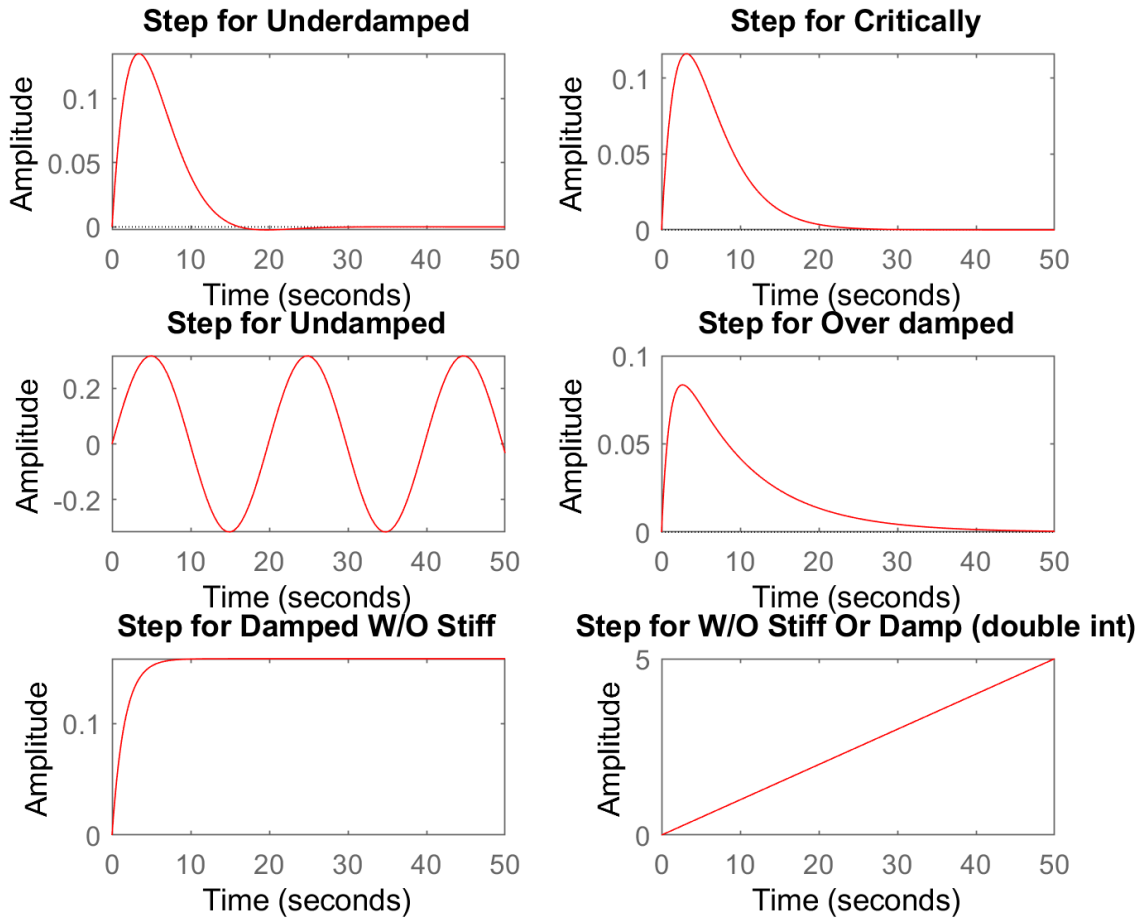


Figure 6 Velocity response of mass spring damper system

The velocity response for a mass spring damper can be seen above for different cases of m , b and k for the mass spring damper system.

The desired control response from the Galen surgical system would ideal be minimal oscillations with a fast response time with limited impedance and damping. Therefore, from the 6 systems observed, a balance between underdamped and critically damped would help us achieve our desired results. In that sense it would be best to keep the stiffness low, and certainly avoid inserting anymore stiffness into the system besides the expected plant response, human impedance, and environment impedance. From these plant observations, damping has the greatest effect on the steady state response and the rise time, as such we expect to see b_{ad} affect the response of the admittance controller more strongly than m_{ad} .

6. Key Terms/Abbreviations:

ff – feedforward with feedback and linearization
fb – feedback alone
MSD – Mass spring underdamped system
MSCD – Mass spring critically damped system
MSUD – Mass spring undamped system
MSOD – Mass spring overdamped system
MD – Mass damper only system
M – Mass only system

7. Normalized Stability analysis of Plant dynamics with an applied admittance controller and impedance bounds

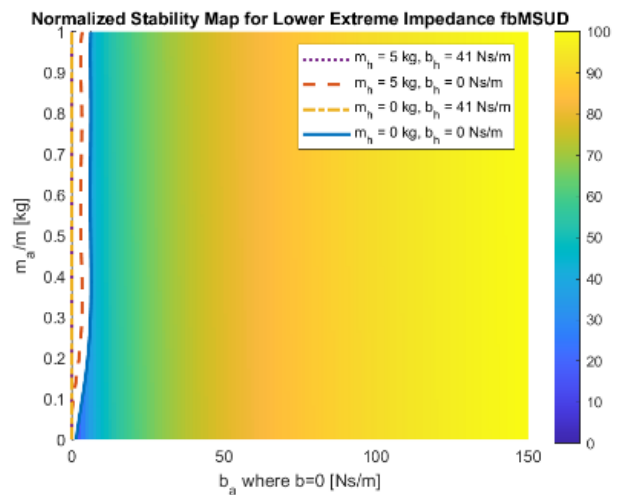
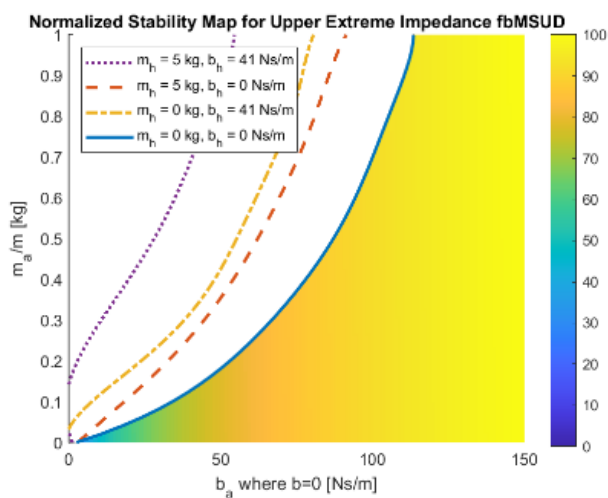
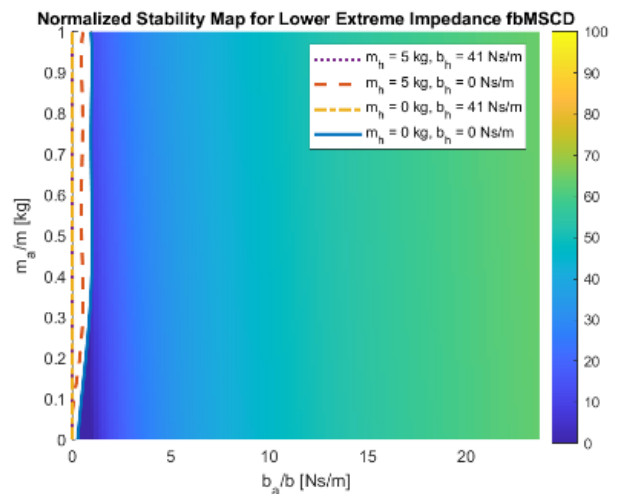
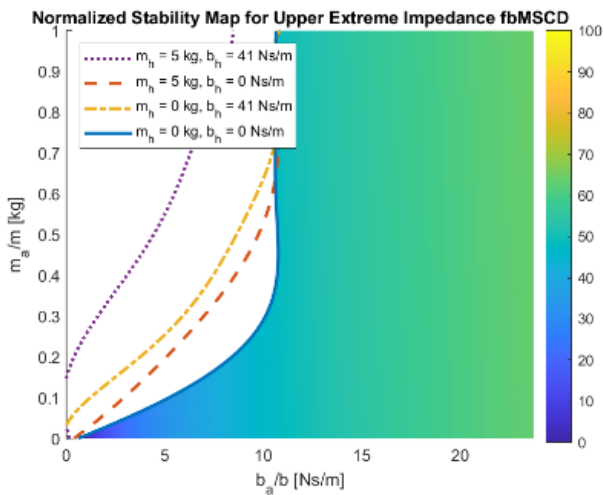
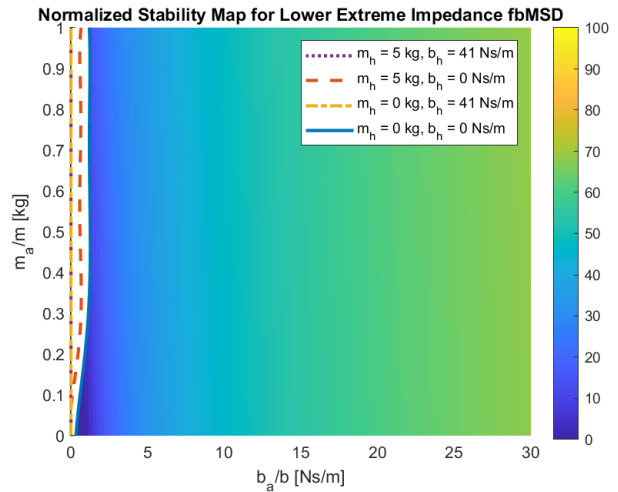
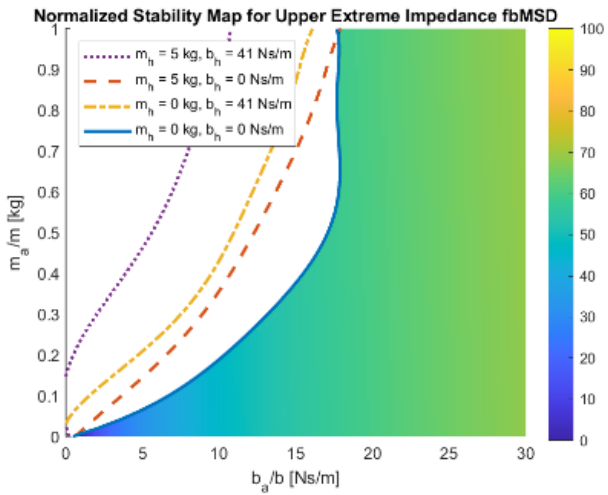
In the following sections 8 and 9, we built impedance maps in the same manner from Aydin et al. (2020) using the stability evaluation method from Stienen et al (2018). These maps highlight the response of all different 6 types of Mass Spring Damper systems identified above. The mass and damping values applied were over a fixed range with a high enough resolution to observe the shape of the stability curve. The max b_{ad} value was 150 and max m_{ad} value was 10. Some of the figures could not be normalized because they already contained no damping or mass and would result in a divide by zero error.

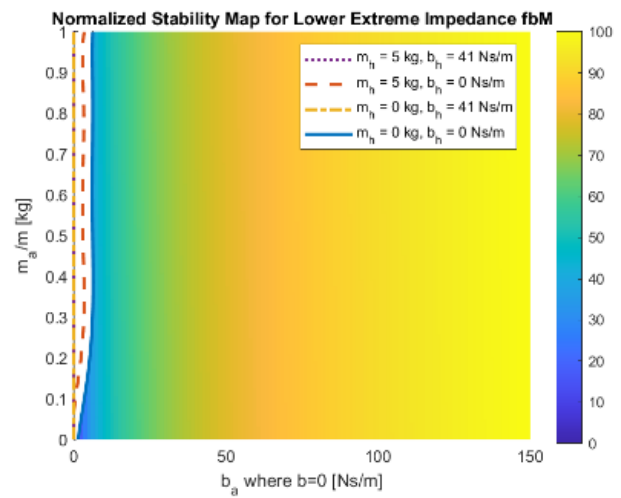
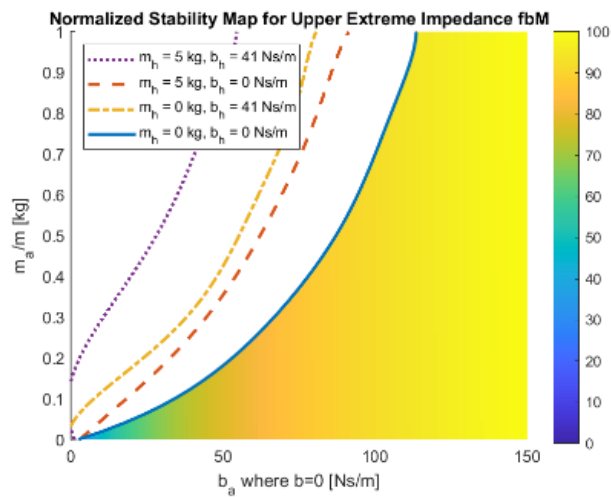
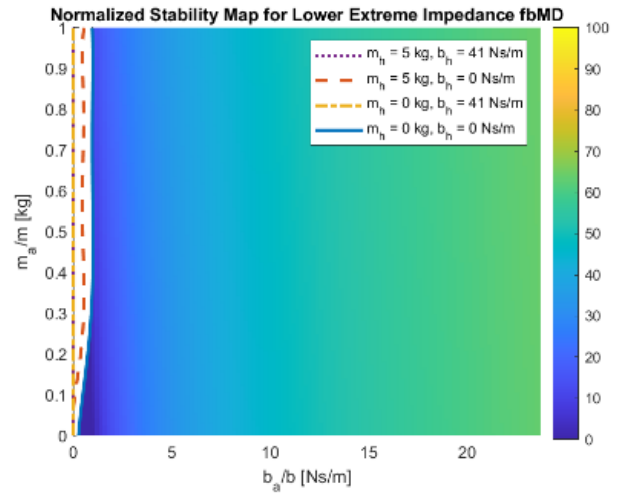
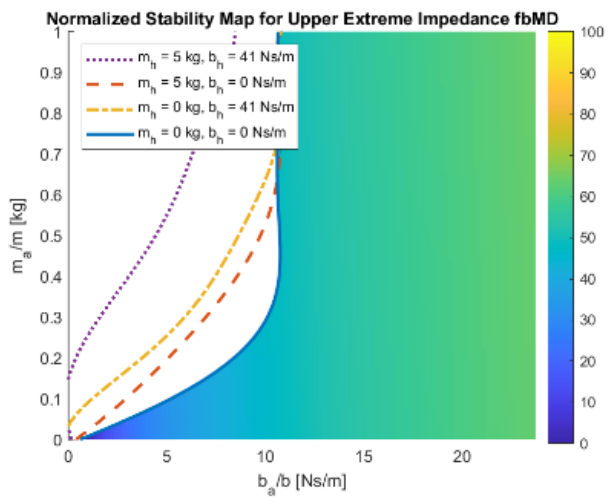
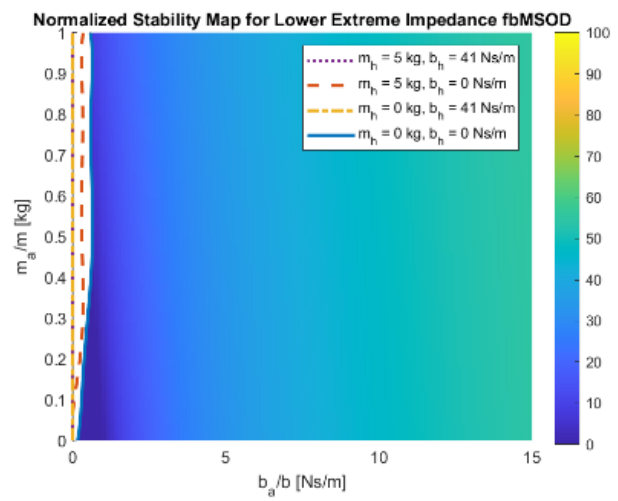
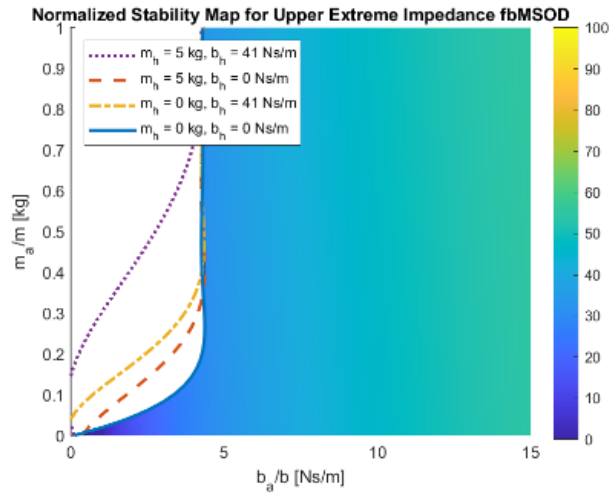
To understand the figures, observe the figures on the left in right together. These figures represent the given plant dynamics explained in the abbreviations section above. On the left is the resultant stability map of the given plant under the response of human impedance and environment impedance given by the same bounds explained in Aydin et al. (2020). On the right explains the plant under the same input but without environment impedance present. Imagine interacting with the mass spring damper, but not making contact with any surfaces or table etc. The human arm is still involved. These figures show the areas where the mass spring damper will stay stable with different values of human interaction. The colored areas, areas that go from blue to yellow, are areas deemed reliably stable for acceptable m_{ad} and b_{ad} values. Areas in white are not stable.

The significance of the color representation of the area of the stable region defines the relative transparency. That is the perceived transparency the human would feel. The more blue, the more transparent or lighter and less impeding the robot feels. If more yellow or orange the robot feel more heavy and less responsive. The non-normalizable figures do not show this very well because they could not reasonably be normalized, but are still rather transparent themselves. However, the most optimal system choices are the MSCD and MSUD systems. Therefore, those systems should be highlighted and investigated more thoroughly since they will more closely represent our true system.

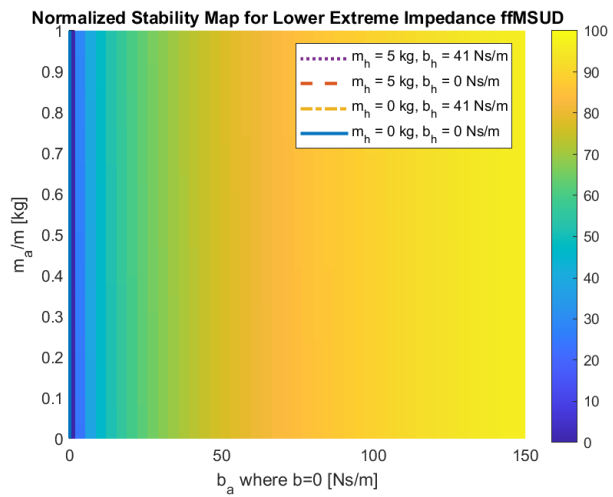
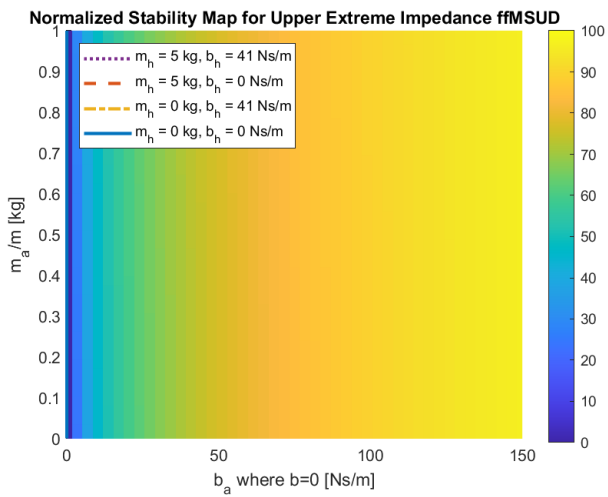
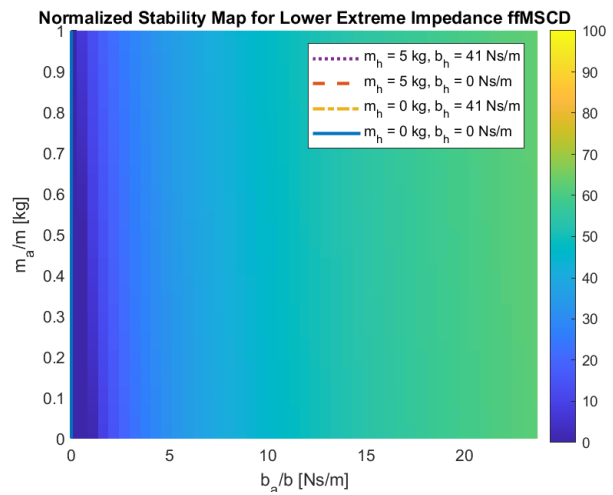
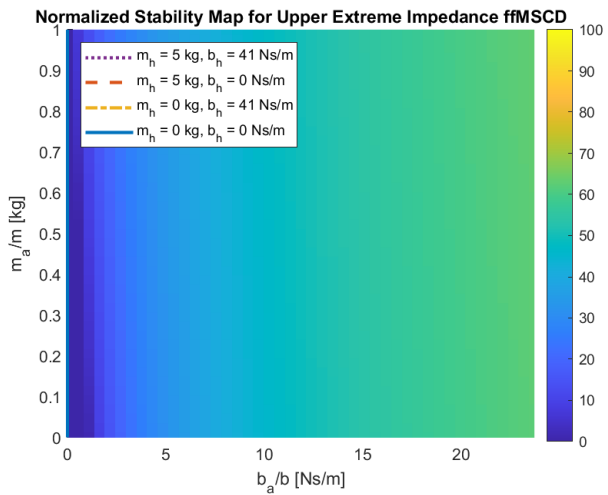
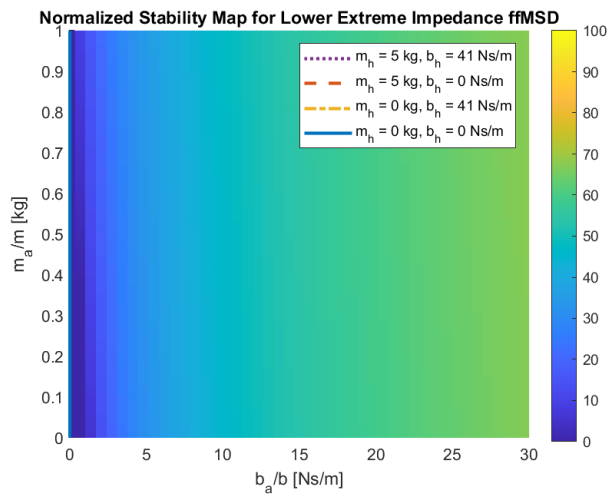
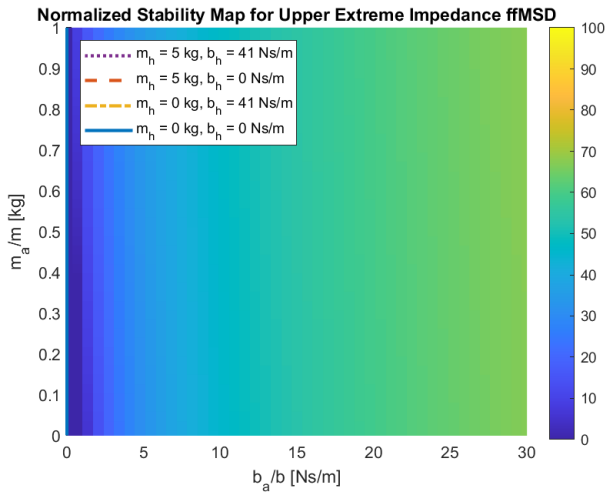
Note that the feedforward plants all seem to represent a much higher level of stability than the feedback systems. This is because we are failing to analyze internal stability, disturbance, noise, and gravity factors, that would quickly lessen the quality of these maps for a feedforward based design. Therefore, the more robust and sure feedback style controllers have been chosen, but more work in the future could be done to investigate a feedforward design. The data for these figures is stored in Normalized_MSD_Phase_margin_Stability_tests folder.

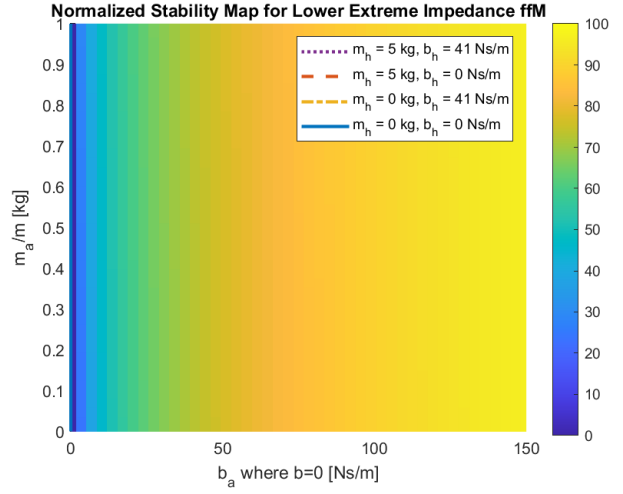
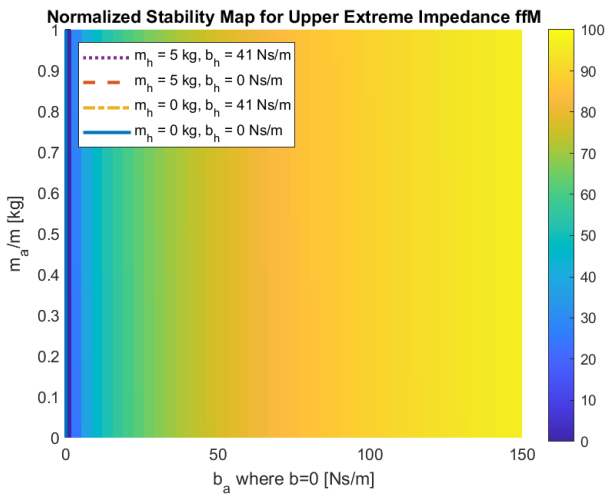
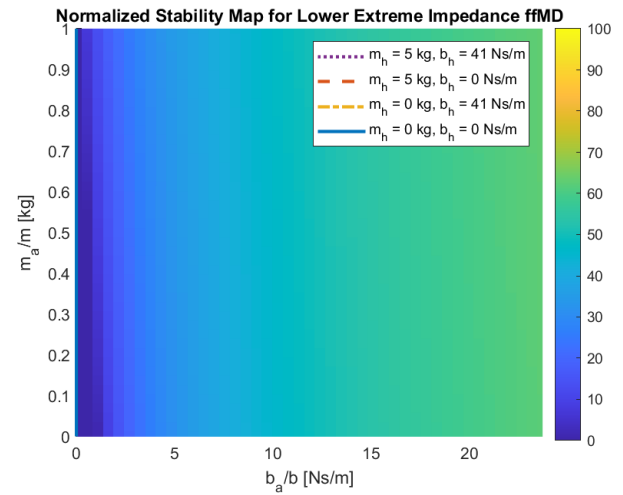
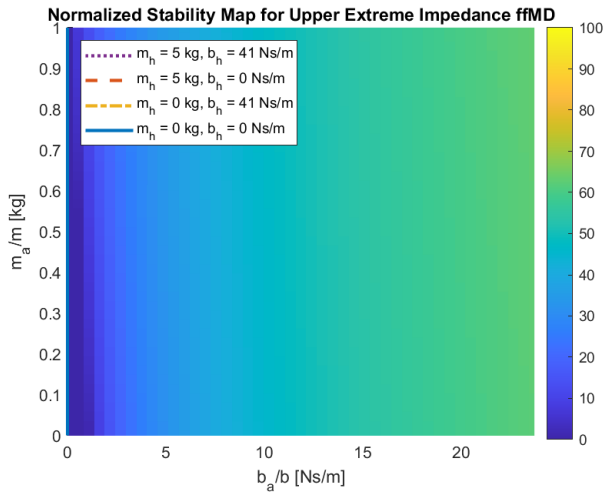
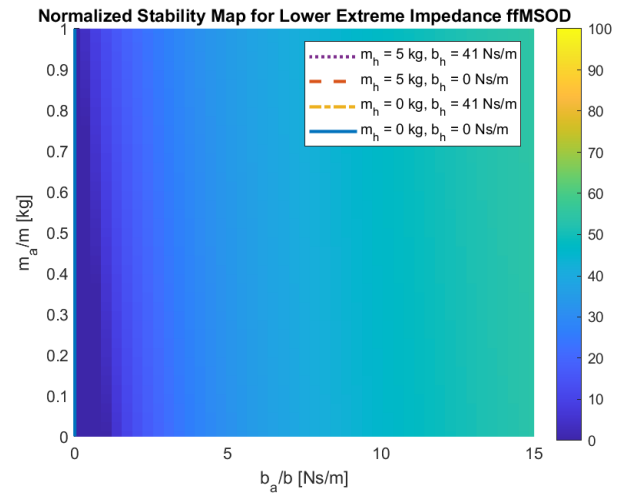
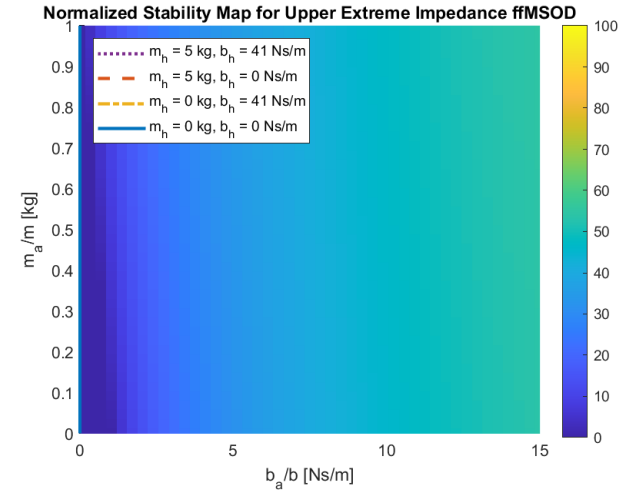
8. Normalized Stability Results: Feedback





9. Normalized Stability Results: Feedback with Feedforward and Linearization





References

1. Aydin, Y., Sirintuna, D., & Basdogan, C. (2020). Towards collaborative drilling with a Cobot using admittance controller. *Transactions of the Institute of Measurement and Control*, 43(8), 1760–1773. <https://doi.org/10.1177/0142331220934643>
2. Keemink AQ, van der Kooij H, Stienen AH. Admittance control for physical human–robot interaction. *The International Journal of Robotics Research*. 2018;37(11):1421-1444. doi:10.1177/0278364918768950

Appendix A

Admittance

$$A(s) = \frac{1}{m_{ad}s + b_{ad}}$$

Plant variations

$$P_1(s) = \frac{1}{ms^2 + bs + k} \text{ Position}$$

$$P_2(s) = \frac{s}{ms^2 + bs + k} \text{ Position derivative -> Velocity}$$

$$P_3(s) = \frac{1}{ms + b} \text{ Velocity no stiffness}$$

Impedance

$$Z_{eq}(s) = mhs^2 + bhs + \frac{kh}{s} + \frac{ke}{s}$$